Mouse CHD4-NURD is Required for Neonatal Spermatogonia Survival and Normal Gonad Development.

Rodrigo Orlandini de Castro (decastror@omrf.org)
OMRF: Oklahoma Medical Research Foundation https://orcid.org/0000-0001-6146-3760
Luciana Previato
OMRF: Oklahoma Medical Research Foundation
Agustin Carbajal
OMRF: Oklahoma Medical Research Foundation
Victor Goitea
OMRF: Oklahoma Medical Research Foundation
Courtney T. Griffin
OMRF: Oklahoma Medical Research Foundation
Roberto J. Pezza
OMRF: Oklahoma Medical Research Foundation https://orcid.org/0000-0003-0279-5516

Research Article

Keywords: mouse gametogenesis, spermatogonia, chromatin remodeling, NURD.

Posted Date: January 11th, 2022

DOI: https://doi.org/10.21203/rs.3.rs-1160749/v1

Abstract

Testis development and sustained germ cell production in adults rely on the establishment and maintenance of spermatogonia stem cells and their proper differentiation into spermatocytes. Chromatin remodeling complexes regulate critical processes during gamete development by restricting or promoting accessibility of DNA repair and gene expression machineries to the chromatin. Here, we investigated the role of CHD4 and CHD3 catalytic subunits of the NURD complex during spermatogenesis. Germ cell-specific deletion of Chd4 early in gametogenesis, but not Chd3, resulted in arrested early gamete development due to failed cell survival of neonate undifferentiated spermatogonia stem cell population. Candidate assessment revealed that CHD4 controls expression of Dmrt1 and its downstream target Plzf, both described as prominent regulators of spermatogonia stem cell maintenance. Our results show the requirement of CHD4 in mammalian gametogenesis pointing to functions in gene expression early in the process.

Introduction

Defects in gametogenesis are a leading cause of infertility and an important cause of birth defects associated with aneuploidy. Insights into the mechanisms underlying testis formation, including spermatogonia stem cell, are necessary to improve the outcomes of common gonad developmental diseases.

In mice, spermatogenesis begins from isolated germ cells called spermatogonia A-singles (As) that undergo to a series of mitotic divisions to produce spermatogonia known as paired (Apr) and aligned (Aal) that contains chains of 4 to 16 cells anchored by intercellular bridges as a result of incomplete cytokinesis [1, 2]. At this point, spermatogonia cells start a process of differentiation (A1, A2, A3, A4 or intermediate (In)), formation of type B spermatogonia, and then transition to pre-leptotene cells that initiate the series of meiotic divisions that ultimately originate spermatozoa.

Chromatin undergoes extensive remodeling during gametogenesis, leading to altered gene expression and chromosome organization, and ultimately controlling obligatory developmental transitions such as the conversion from undifferentiated to differentiated spermatogonia, spermatogonia commitment to meiosis, and meiotic progression [3, 4]. The NURD (NUcleosome Remodeling and Deacetylase) is a prominent chromatin modifying complex that functions to control gene expression via chromatin remodeling and histone deacetylation [5, 6]. The NURD complex contains two highly conserved and widely expressed catalytic subunits, CHD3/Mi-2α (chromodomain-helicase-DNA-binding 3) and CHD4/Mi-2β, which are members of the SNF2 superfamily of ATPases [5–9]. NURD plays a central role in various developmental and cellular events, such as controlling the differentiation of stem cells, maintaining cell identity, and responding to DNA damage [9–11]. In testis, CHD5 is required for normal spermiogenesis and proper spermatid chromatin condensation [12], while CHD3/4 has been described to localize at the X-Y pseudoautosomal region, the X centromeric region, and then spreads into the XY body chromatin [13, 14]. Although the role of CHD5 has been well defined, the requirements and mechanisms of CHD4 and

CHD3 in mouse gametogenesis and testis development is not completely understood. In a recent work, siRNA knockdown of CHD4 in primary cultures followed by spermatogonia transplantation revealed a loss of the regenerative capability of these cells. Interpretation of RNA-seq data obtained from spermatogonia siRNA treated versus control cell cultures revealed global transcription changes, including genes possibly involved in cell self-renewal [15]. Questions remain unanswered regarding the effect of direct Chd3 and Chd4 deletion in germ cells and testis development.

In this study, we report that testis-specific specific deletion of CHD4 (but not CHD3) is essential for testis development and sustained germ cell production. This germ cell-specific deletion of CHD4 results in the developmental arrest of undifferentiated spermatogonia in neonatal mice progressing to a Sertoli-only phenotype. Our studies of selected CHD4 target genes and subsequent cytological and expression analysis show that CHD4 control Dmrt1 gene expression and downstream targets such as Plzf. We propose these results suggest a possible mechanism by which CHD4 contributes to early germ cell development regulating genes that are required for survival/maintenance of spermatogonia cells.

Results

Chd4 expression during mouse germ cell development

To investigate a potential role for CHD4 in germ cells, we assessed CHD4 expression in newborn and adult mouse testes by immunofluorescence. CHD4 was highly expressed in spermatogonia cells (marked by PLZF, aka ZBTB16) and in Sertoli cells (marked by SOX9) (Fig. 1A and Fig. S1) but not in the negative control (PLZF-positive spermatogonia from Ddx4-*Chd4*$^{-/-}$ testes, Fig. S2A). PLZF is expressed in undifferentiated spermatogonia [16, 17] (Fig. 1A). In agreement with a previous report [13], immunosignal of CHD4 was detected in late-pachytene stages (Fig. 1A, selected area on adult mouse top panel). In sum, CHD4 is detected in spermatogonia, Sertoli cells, and primary spermatocytes.

We confirmed that CHD4 is expressed at pre-meiotic stages of male gamete development by analyzing CHD4 protein levels by western blot in enriched fractions (see methods for details) of undifferentiated and differentiating spermatogonia (obtained from wild type 7dpp mice and using THY1.2+ and c-KIT+ affinity columns, respectively) (Fig. 1B). CHD4 was also detected in the affinity column flowthrough (which was enriched mostly in Sertoli cells, here demonstrated by immunoblotting of Sox9). The level of cell population enrichment was assessed by western blot and markers specific for undifferentiated spermatogonia (PLZF) and differentiating spermatogonia (STRA8) (Fig. 1B). Additionally, we analyzed cell fractions enrichment by immunofluorescence (Fig. S3).

Composition of CHD4-NURD complexes during spermatogenesis

NURD function is influenced by its subunit composition [18, 19]. To determine whether the expression of NURD composition might change during spermatogenesis, we analyzed the levels of representative NURD

subunits in enriched fractions of undifferentiated and differentiating spermatogonia, as well as in the flow-through (enriched in Sertoli cells) after spermatogonia enrichment. NURD subunits HDAC2A, MTA1, RBBP4, RBBP7 and MBD2 were present in enriched fractions of undifferentiated (THY1.2+) and differentiating (c-KIT+) spermatogonia (Fig. 1B), suggesting a particular composition and perhaps a different function for CHD4-NURD in this cell type.

To determine the composition of CHD4-NURD complexes, we used co-immunoprecipitation analysis to uncover NURD subunits that interact with CHD4 in enriched fractions of THY1.2 and c-KIT spermatogonia cells together and the flow-through. The NURD subunits HDAC2A, MTA1, and RBBP4/RBBP7, but not MBD2, coimmunoprecipitated with CHD4 from all fractions (Fig. 1C). HDAC2A coimmunoprecipitated with CHD4 from wild type and *Chd3*$^{-/-}$ spermatogonia cells (Fig. S2B). These data suggest that: i) CHD4 forms a NURD complex independently of CHD3, ii) that loss of CHD3 does not perturb CHD4-NURD complex formation in spermatogonia cells.

Deletion of Chd4 **but not** Chd3 **results in testis developmental defects**

To examine the potential functions of *Chd4* and *Chd3* during spermatogenesis, we generated a series of *Chd4* and *Chd3* germline conditional knockout mice (Fig. 2). To delete the floxed allele in gonocytes (embryonic day 15.5, Fig. 2C) [20], male Ddx4-Cre; *Chd4*$^{WT/\Delta}$ were crossed with *Chd4*$^{fl/fl}$ females to generate Ddx4-Cre; *Chd4*$^{fl/\Delta}$ conditional knockout mice (here called Ddx4-*Chd4*$^{-/-}$) (Fig. 2A). A similar strategy was used to generate Ddx4-*Chd3*$^{-/-}$ mice (Fig. 2B).

Ddx4-*Chd4*$^{-/-}$ adult mice (2 months old) appeared normal in all aspects except in the reproductive tissues. Testes were significantly smaller in Ddx4-*Chd4*$^{-/-}$ males (mean: 0.017g ± SD: 0.005, number of quantified mice n = 4 (8 testes), P≤0.0001, t test) compared to wild type (0.104 g ± 0.015, n = 6 mice (12 testes)) littermates (Fig. 2C and D), indicating severe developmental defects in the testis. We confirmed deletion of *Chd3* and *Chd4* by RT-qPCR (Fig. 2E). Immunofluorescence analysis of neonatal Ddx4-*Chd4*$^{-/-}$ testis CHD4 was absent at 1ddp (Fig. S2A).

We found that adult Ddx4-*Chd4*$^{-/-}$ males develop testicular hypoplasia with hyperplasia of interstitial cells and lack spermatozoa (Fig. 3A). The number of seminiferous tubules is similar between wild type and mutant animals, but the diameter is reduced (wild type, mean ± SD, 287 ± 34, n=400 seminiferous tubules cross sections (3 different mice, 2-month-old) versus *Chd4*$^{-/-}$ 148 ± 21.3, n=210, P<0.0001 t test).

Analysis of Ddx4-*Chd4*$^{-/-}$ testes revealed a total loss of germ cells (marked by TRA98) in seminiferous tubules (Fig. 3B). No developing gametes were observed, including cell types at early stages (e.g., spermatogonia) (Fig. 3A and B). Sertoli cells develop normally in Ddx4-*Chd4*$^{-/-}$ mice, consistent with the specific loss of *Chd4* in germ cells at early stages of development. We did not observe differences in germ cell development between wild type and Ddx4-*Chd3*$^{-/-}$ mice (Fig. S3), consistent with their similar testis sizes (Fig. 2C and D).

We also analyzed H&E-stained histological sections of ovaries from 45-day-old wild type and Ddx4-*Chd4*$^{-/-}$ female mice. We noted a significant reduction in ovary size, an increase in stromal cells, a reduced number of follicles (wild type, 10 ± 3, n=6 mice versus Ddx4-*Chd4*$^{-/-}$ 0.6 ± 0.9, n=5, P<0.0001 t test) and absent corpora lutea (wild type, 9 ± 1, n=6 mice versus Ddx4-*Chd4*$^{-/-}$ 0 ± 0, n=5, P<0.0001 t test) in the Ddx4-*Chd4*$^{-/-}$ mice compared to wild type (Fig. 3C).

We conclude that deletion of *Chd3* has no apparent effect on gamete development. However, germ cell specific deletion of *Chd4* results in severe male and female germ cell developmental defects, possibly originated at premeiotic stages of development.

CHD4 is required for neonate spermatogonia survival

The severe phenotypes observed in Ddx4-*Chd4*$^{-/-}$ mice (Fig. 2 and 3) prompted us to investigate spermatogonial differentiation during testis development in newborns. Testis sections from 9 dpp Ddx4-*Chd4*$^{-/-}$ mice stained with H&E showed a markedly reduced number of germ cells (Fig. 4A) as well as differences in cell composition, compared to those from age-matched wild type mice. To analyze this in detail, we examined the presence of cells expressing STRA8 (Fig. 4A), which marks differentiating spermatogonia, SYCP3 and yH2AX which are markers of primary spermatocytes and TRA98, a marker for germ cells (Fig. S5). Whereas tubules from 9 dpp wild type mice contained cells expressing TRA98 (45 ± 10, n=66 seminiferous tubules counted obtained from 3 mice) and STRA8 (18.8 ± 8.4, n=36 obtained from 3 mice), tubules from *Chd4*$^{-/-}$ mice showed a near absence of cells expressing these markers (TRA98 4.6 ± 3, n=60 obtained from 3 mice, P<0.0001, t test; STRA8 2.5 ± 3.5, n=42 obtained from 3 mice, P<0.0001, Student t test) (Fig. 4A). Testes sections from 9 dpp *Chd4*$^{-/-}$ mice also showed a reduction in primary spermatocytes expressing the meiotic prophase I markers SYCP3 and γH2AX compared to those from 9 dpp wild type mice (Fig. S5A and B). Together, the results further suggest that testis defects in *Chd4*$^{-/-}$ mice begin early, during pre-meiotic stages of postnatal development, leading to an absence of germ cells in adults.

To pinpoint when the testes defects originate in *Ddx4-Chd4*$^{-/-}$ mice, we stained testes sections from 1-21 dpp mice for the expression of TRA98 (all germ cells). We observe that as general trend, in all analyzed stages, the number of TRA98 positive cells was reduced in *Chd4*$^{-/-}$ mice compared to wild type, progressing to total absence of germ cells (Fig. S6). *Chd4* mutant sections displayed a small reduction in the number of cells expressing TRA98 at both 1dpp and 3dpp (Fig. 4B and 4C and Fig. S6). We observed equal numbers of SOX9-positive Sertoli cells in testes from wild type and *Chd4*$^{-/-}$ mice at 3, 4, and 7 dpp (Fig. 4C), as expected for the specific loss of *Chd4* in spermatogonia cells. Both PLZF-positive and TRA98-positive cells were substantially reduced in *Chd4*$^{-/-}$ testis compared to wild type testis at 4 dpp and 7dpp (Fig. 4C).

Given that Chd4 may act as a regulator of cell-cycle progression, we then examined whether the rapid loss of PLZF-positive neonate spermatogonia in *Chd4*$^{-/-}$ testes was due to altered proliferative activity. We conducted EdU incorporation study to test this possibility. 4 dpp mice were injected with EdU and

analyzed 3 h later, after which we assayed its incorporation in PLZF-positive spermatogonia in whole mounts of seminiferous tubules (Fig. S7A). We found that spermatogonia cell proliferation (PLZF/EdU^{+} cells) in wild type and Ddx4-Chd4$^{-/-}$ is proportionally the same (Fig. S7C). In addition, reduced amount of total PLZF-positive cells was found in Ddx4-CHD4$^{-/-}$ compared to wild type in the whole-mounting experiment (Fig. S7B).

To determine whether cell death contributed to the loss of Ddx4-*Chd4*$^{-/-}$ neonate spermatogonia (Fig. 4C), we performed TUNEL assay in staining paraffin embedded testis sections of wild type and *Chd4*$^{-/-}$ four days old testis. At this age the testis is mostly constituted by spermatogonia and Sertoli cells, which can be easily distinguished by DAPI nuclear staining patterns. We found a significant increase in the percentage of apoptotic cells in *Chd4*$^{-/-}$ testis compared to wild type mice (Fig. 4D).

We conclude that the possible cause of spermatogonia failure in *Chd4*$^{-/-}$ mice is in the survival/maintenance of neonate undifferentiated spermatogonia.

CHD4, DMRT1, and PLZF work together in a regulatory axis involved in spermatogonia cell survival

Our results show that CHD4 is required for spermatogonia maintenance/survival. We then reason that CHD4 may interact with genes that have been described to work in spermatogonia maintenance. Indeed, DMRT1 has been show to function in spermatogonia stem cells maintenance, and this function seems to be mediated by direct regulation of Plzf gene expression, another transcription factor required for spermatogonia maintenance [21]. To test our hypothesis, we immunostained paraffined testes sections from 1, 4, and 7 dpp mice for the presence of DMRT1 (Fig. 5A and B). Compared to wild type, *Chd4* mutant showed a clear reduction in DMRT1 immunosignal.

Recent work described that Dmrt1 controls Plzf expression, which is a transcription factor required for spermatogonia maintenance [21]. We then tested the effect of CHD4 depletion in Plzf expression. PLZF immunostaining of testes sections from 1, 4, and 7 dpp mice revealed a significantly reduction of this protein in Chd4 knockout cells respect to wild type (Fig. 5C and D). This is consistent with a model by which CHD4 control of Dmrt1 and downstream targets influences cell survival/maintenance (Fig. 5E).

We concluded that Chd4 participates in the maintenance/survival of neonate spermatogonia stem cell possibly through transcriptional regulation of genes participating in these critical processes. We note, however, that the dramatic phenotype observed in CHD4$^{-/-}$ spermatogonia likely reflect CHD4 targeting a wide spectrum of genes participating in different pathways.

Discussion

In this work, we examined the potential function of two critical NURD catalytic subunits, CHD4 and CHD3, in spermatogenesis. Our data suggest that a CHD4-NURD (but not CHD3-NURD) complex controls neonate spermatogonia development at early stages of testis development. Germline deletion of *Chd4*,

but not *Chd3*, results in a severe loss of germ cells specifically at early stages of the testis cord development. *Chd4* deletion affects spermatogonia, with the first obvious consequences in undifferentiated spermatogonia. Our results agree with a recent report, in which using a in vitro approach, knockdown of CHD4 in spermatogonia cultures followed by cell transplantation in cell-ablated recipient testis, resulted in reduced viability of undifferentiated spermatogonia [15].

Most CHDs are expressed in testis; however, their insertion into the NURD complex seems to be developmentally regulated, with apparent different patterns of expression during gametogenesis. CHD5 [7–9] has been shown to be expressed and required to compact chromatin in postmeiotic stages of spermatogenesis [12, 22]. Our results show that CHD4 is expressed and functions at premeiotic stages of gametogenesis.

The functions of CHD4-NURD in neonate spermatogonia development and male gametogenesis are further revealed by our cytological analysis showing that CHD4 dowregulates the expression of Dmrt1 (Fig. 5). DMRT1 function in maintenance of spermatogonia stem cells has been proposed to be mediated by direct regulation of Plzf gene expression, another transcription factor required for spermatogonia maintenance [21]. In agreement with this possibility, we observed that the amount of PLZF was significantly reduced in Chd4 knockout versus wild type cells. In sum, our work provides evidence of a regulatory axis in which CHD4 may control important genes involved in spermatogonia stem cell maintenance and survival. The effect we observed with CHD4 deletion on Dmrt1 expression in spermatogonia (and possibly downstream genes such as Sohlh1) is in contrast with a recent report showing an increase in Dmrt1 and Sohlh1 expression measured by scRNA-seq in Chd4 siRNA treated (knockdown) cultured spermatogonia cells [15]. These contrasting results, and some of their implications, such as on the primary function of CHD4 as an activator of genes involved in spermatogonia survival, may be assigned to differences in the experimental system or experimental approaches utilized. Additional work will be required to test Sohlh1 expression level in CHD4 knockout spermatogonia, another Dmrt1 direct target involved in cell survival and differentiation [21, 23, 24], as well as in the Stra8 gene, the latter which precocious expression is detected in Dmrt1 knockout mice. We note that the dramatic cellular phenotype we observed after CHD4 depletion in spermatogonia may be more accurately explained by CHD4 activity targeting several genes and different pathways.

Material And Methods

Mice

CHD4-floxed mice (*CHD4*$^{fl/fl}$) have been described [25]. *Chd3*-floxed mice were generated by Cyagen Biosciences using homologous recombination of a targeting vector in C57Bl/6 embryonic stem cells. The targeting vector incorporated a 5’ LoxP site inserted between exons 12 and 13 and a 3’ LoxP site inserted between exons 20 and 21 of the wild type *Chd3* allele. Transgenic *Cre* recombinase mice *Ddx4-Cre*$^{FVB\text{-}Tg(Ddx4\text{-}cre)1Dcas/J}$ was purchased from The Jackson Laboratory (Bar Harbor, ME). *Chd3 or Chd4* gonad-

specific knockouts and wild-type heterozygotes littermates were obtained from crosses between female homozygous *flox/flox* mice with male heterozygous Cre/+; *Chd3* Wt/flox and/or *Chd4* Wt/flox mice.

All experiments conformed to relevant regulatory standards guidelines and were approved by the Oklahoma Medical Research Foundation-IACUC (Institutional Animal Care and Use Committee).

Mice Genotyping

Characterization of wild type and *floxed* alleles was carried out by PCR using the following oligonucletides: CHD3 forward 5'-GGGTGGAGGTGGAAAGTGTA, CHD3 reverse 5'-AGAGGACAGGTCACAGGACAA, CHD4 forward 5'- TCCAGAAGAAGACGGCAGAT and CHD4 reverse 5'-CTGGTCATAGGGCAGGTCTC. The presence of *cre* recombinase allele were determine by PCR using the following primers: DDX4-Cre forward 5'-CACGTGCAGCCGTTTAAGCCGCGT, DDX4-Cre reverse 5'-TTCCCATTCTAAACAACACCCTGAA.

Real time-PCR

Total RNA was isolated from adult testis or from enriched fractions of spermatogonia with the Direct-zol RNA MiniPrep Plus kit (Zymo Research). RNA (2.0µg) was oligo-dT primed and reverse-transcribed with the high-capacity RNA-to-cDNA kit (Applied Biosystems). Exon boundaries of *Chd4 and Chd3* were amplified using TaqMan Assays (Applied Biosystems) as directed by the manufacturer using Beta-2 macroglobulin as standard. TaqMan Mm01190896_m1 (Chd4), Mm01332658_m1 (Chd3), and Mm00437762_m1 (Beta-2 microglobulin). Gene expression was normalized with respect to wild type with wild type expression levels considered to be 1.

Western blot cell lysates

Total testis or enriched cells fractions were lysed in ice-cold protein extraction buffer containing 0.1% Nonidet P-40, 50 mM Tris-HCl, pH 7.9, 150 mM NaCl, 3 mM MgCl2, 3 mM EDTA, 10% glycerol, 1 mM DTT, 1mM PMSF and protease inhibitors (ThermoFisher Scientific, A32965) followed by sonication (3 pulses of 10 seconds) using micro ultrasonic cell disrupter (Kontes). The relative amount of protein was determined measuring absorbance at 260nm using NanoDrop 2000c spectrophotometer (ThermoFisher Scientific). Proteins were solubilized with 2X sample buffer (4% SDS, 160 mM Tris-HCl, pH 6.8, 20% glycerol, 4% mM β-mercaptoethanol, and 0.005% bromophenol blue) and 30 µg/lane of sample were separated by 4–15% gradient Tris-acetate SDS-PAGE and electro transferred to PVDF membrane (Santa Cruz Biotechnology, sc-3723). The blots were probed with individual primary antibodies, and then incubated with HRP-conjugated goat anti-mouse or rabbit antibody as required. In all blots, proteins were visualized by enhanced chemiluminescence, and images acquired using Western Blot Imaging System c600 (Azure Biosystems). ImageJ software were used for quantification of non-saturated bands and α-tubulin were used for normalization. Antibodies used are detailed in table S1.

Histology and immunostaining

Testes and ovaries were dissected, fixed in 10% neutral-buffered formalin (Sigma) and processed for paraffin embedding. After sectioning (5–8-µm), tissues were positioned on microscope slides and analyzed using hematoxylin and eosin using standard protocols. For immunostaining analysis, tissue sections were deparaffinized, rehydrated and antigen was recovered in sodium citrate buffer (10 mM Sodium citrate, 0.05% Tween 20, pH 6.0) by heat/pressure-induced epitope retrieval. Incubations with primary antibodies were carried out for 12 h at 4°C in PBS/BSA 3%. Primary antibodies used in this study are detailed in table S6 Following three washes in 1 X PBS, slides were incubated for 1 h at room temperature with secondary antibodies. A combination of fluorescein isothiocyanate (FITC)-conjugated goat anti-rabbit IgG (Jackson laboratories) with Rhodamine-conjugated goat anti-mouse IgG and Cy5-conjugated goat anti-human IgG each diluted 1:450 were used for simultaneous triple immunolabeling. Slides were subsequently counterstained for 3 min with 2 µg/ml DAPI containing Vectashield mounting solution (Vector Laboratories) and sealed with nail varnish. We use Zen Blue (Carl Zeiss, inc.) for imaging acquisition and processing.

Enrichment of Spermatogonia Populations

Our procedure of cell enrichment followed [26, 27]. Briefly, testis from 7 dpp mice (or any other indicated age) were removed from mice and placed in a Petri dish containing Dulbecco's Modified Eagle Medium (DMEM without phenol red). After detachment of the tunica albuginea, the seminiferous tubules were loosen using forceps and incubated in a 15 ml tube containing DMEM containing 1 mg/mL of collagenase, 300 U/mL of hyaluronidase and 5 mg/mL DNAse I (StemCell Technologies) under gentile agitation for 10 min. The seminiferous tubule clumps were pelleted by gravity and the cell suspension containing interstitial cells was discarded. The tubules were then incubated of with 0.05% Trypsin-EDTA solution (Mediatech Inc) for 5 min and the reaction was stopped by adding 10% volume of 10% BSA in PBS. Single cell suspension was obtained by mechanical resuspension followed by filtration through a 40-µm-pore-size cell strainer and dead cells were removed using Dead Cell Removal Kit (Miltenyi Biotec 130-090-101). Differentiating c-KIT+ neonate spermatogonia cells were magnetically labeled with CD117 (c-KIT+) MicroBeads (Miltenyi Biotec 130-091-224) and isolated using MS columns (Miltenyi Biotec 130-042-201) according to manufacturer’s instructions. After the depletion of the c-KIT+ cells, the population of undifferentiated neonate spermatogonia cells were separated using CD90.2 (THY1.2+) MicroBeads (Miltenyi Biotec 130-121-278). Relative enrichment of cell populations was evaluated by STRA8 (c-Kit fractions) or PLZF (THY1.2 fractions) western blots (Fig. 1B). After c-kit and THY1.2 separation, the flow-through mostly contained Sertoli cells (SOX9 positive, Fig. S3). The number of cells obtained from a pool of 4 mice testis at 7dpp was approximately $3.43x10^5$ in THY1.2 fractions and $5.71x10^5$ in c-Kit fractions.

Immunoprecipitation

Co-immunoprecipitation experiments were performed using testis of wild type or Ddx4-CHD3$^{-/-}$ mouse (Adult - 2 months old). After detunication, seminiferous tubules were loosen using forceps, washed twice with cold PBS and lysed using ice-cold RIPA buffer (50 mM Tris pH 7.5, 150 mM NaCl, 1% NP40, 0.5% Deoxycholate) containing protease inhibitors (ThermoFisher Scientific, A32965), sheared using 23 G

needle, incubated on ice for 15 min and centrifugated at 1000 x g for 10 minutes at 4 ºC. Supernatant were collected in a separate tube, the pellet were resuspended in RIPA buffer, disrupted by sonication (3 pulses of 10 seconds) and centrifuged 12.000 x g. This second supernatant was combined with the previous one and protein concentration was determined. We used 1mg of protein for each immunoprecipitation. Lysates were pre-cleared with protein G magnetic beads (BioRad, 161-4023) for 1 hour at room termperature and incubated with rabbit anti-CHD3 (5µg, Bethyl A301-220A), rabbit anti-CHD4 (2 µg, Abcam ab72418), or rabbit IgG (5µg Jackson ImmunoResearch, 011-000-003). Lysates were rotated overnight at 4 ºC and immune complexes were collected with protein G magnetic beads (2 hours at 4 ºC). Beads were washed 4 times with washing buffer (50 mM Tris pH 7.5, 150 mM NaCl, 0.1% TX100, 5% glycerol) and two times with PBS. Proteins were eluted by boiling the beads with 2X sample buffer and analyzed by SDS-PAGE as described above.

EdU-based proliferation assay

Mice at indicated age received subcutaneous injection of EdU (50 mg/Kg) (Invitrogen, A10044) 3 hours prior euthanasia. After that, testes were removed and processed for whole-mount immunohistochemistry. EdU was detected by incubation of testis samples with reaction mix (2 mM $CuSO_4$, 50 mM ascorbic acid and 2 mM Alexa Azide conjugates (488 or 647) in PBS) for 3 hours at room temperature.

Whole-mount seminiferous tubules

Immunohistochemistry of whole-mount seminiferous tubules was performed as described [28]. Briefly, after detachment of the tunica albuginea, the seminiferous tubules were loosen using forceps and incubated in a 15 ml tube containing DMEM containing 1 mg/mL of collagenase, 300 U/mL of hyaluronidase and 5 mg/mL DNAse I (StemCell Technologies) under gentile agitation for 10 min. The seminiferous tubules clumps were pelleted by gravity and the cell suspension containing interstitial cells was discarded. Seminiferous tubules were fixed for 4h in 4% PFA (pH7.2 in PBS) at 4 ºC. After extensively wash in PBS, the tubules were permeabilized with series of MeOH/PBS (25, 50, 75, 95%, and twice in 100% MeOH) for 15 min at room temperature, treated with MeOH : DMSO : H_2O_2 (4:1:1), and rehydrated with MeOH/PBS (50, 25% and twice in PBS). Samples were incubated in ice-cold blocking solution PBSMT (PBS with 2% non-fat dry milk and 0.5% triton X-100) for 3 hours and then over-night at 4 ºC with indicated primary antibodies under gentle rotation. Seminiferous tubules were washed in PBSMT (5 x 1h) and incubated with dye conjugated (Alexa488 or TRITC) goat anti-mouse or rabbit antibody as required. The tubules were mounted in raised coverslips glass slides.

Statistical Analyses

Results are presented as mean ± standard deviation (SD). Statistical analysis was performed using Prism Graph statistical software. Two-tailed unpaired Student's t-test was used for comparisons between 2 groups. $P < 0.05$ was considered statistically significant.

Declarations

Ethics approval and consent to participate. All experiments conformed to relevant regulatory standards guidelines and were approved by the Oklahoma Medical Research Foundation-IACUC (Institutional Animal Care and Use Committee).

Consent for publication. Not applicable.

Availability of data and materials. All data generated or analyzed during this study are included in this published article [and its supplementary information files].

Competing interest. The authors declare no competing interest.

Funding. NIH/NICHD HD103562 and NIH/NIGMS 125803.

Authors' contribution. ROC performed experiments, analyzed data, wrote, and edited the manuscript. LP performed experiments and edited the manuscript. AC performed experiments, analyzed data, and edited the manuscript. VG analyzed data and edited the manuscript. CJG provided essential material and edited the manuscript. RJP supervised, analyzed data, wrote, and wrote the manuscript**.**

Acknowledgments. Not applicable.

References

1. Greenbaum MP, Yan W, Wu MH, Lin YN, Agno JE, Sharma M, et al. TEX14 is essential for intercellular bridges and fertility in male mice. Proc Natl Acad Sci U S A. 2006;103(13):4982-7. Epub 2006/03/22. doi: 10.1073/pnas.0505123103. PubMed PMID: 16549803; PubMed Central PMCID: PMCPMC1458781.
2. Phillips BT, Gassei K, Orwig KE. Spermatogonial stem cell regulation and spermatogenesis. Philos Trans R Soc Lond B Biol Sci. 2010;365(1546):1663-78. doi: 10.1098/rstb.2010.0026. PubMed PMID: 20403877; PubMed Central PMCID: PMCPMC2871929.
3. Wang L, Xu Z, Khawar MB, Liu C, Li W. The histone codes for meiosis. Reproduction. 2017;154(3):R65-R79. doi: 10.1530/REP-17-0153. PubMed PMID: 28696245.
4. Stanley FK, Moore S, Goodarzi AA. CHD chromatin remodelling enzymes and the DNA damage response. Mutat Res. 2013;750(1-2):31-44. doi: 10.1016/j.mrfmmm.2013.07.008. PubMed PMID: 23954449.
5. Goodarzi AA, Kurka T, Jeggo PA. KAP-1 phosphorylation regulates CHD3 nucleosome remodeling during the DNA double-strand break response. Nat Struct Mol Biol. 2011;18(7):831-9. doi: 10.1038/nsmb.2077. PubMed PMID: 21642969.
6. Larsen DH, Poinsignon C, Gudjonsson T, Dinant C, Payne MR, Hari FJ, et al. The chromatin-remodeling factor CHD4 coordinates signaling and repair after DNA damage. J Cell Biol. 2010;190(5):731-40. doi: 10.1083/jcb.200912135. PubMed PMID: 20805324; PubMed Central PMCID: PMCPMC2935572.

7. Pan MR, Hsieh HJ, Dai H, Hung WC, Li K, Peng G, et al. Chromodomain helicase DNA-binding protein 4 (CHD4) regulates homologous recombination DNA repair, and its deficiency sensitizes cells to poly(ADP-ribose) polymerase (PARP) inhibitor treatment. J Biol Chem. 2012;287(9):6764-72. doi: 10.1074/jbc.M111.287037. PubMed PMID: 22219182; PubMed Central PMCID: PMCPMC3307306.
8. Polo SE, Kaidi A, Baskcomb L, Galanty Y, Jackson SP. Regulation of DNA-damage responses and cell-cycle progression by the chromatin remodelling factor CHD4. EMBO J. 2010;29(18):3130-9. doi: 10.1038/emboj.2010.188. PubMed PMID: 20693977; PubMed Central PMCID: PMCPMC2944064.
9. Clapier CR, Cairns BR. The biology of chromatin remodeling complexes. Annu Rev Biochem. 2009;78:273-304. doi: 10.1146/annurev.biochem.77.062706.153223. PubMed PMID: 19355820.
10. Torchy MP, Hamiche A, Klaholz BP. Structure and function insights into the NuRD chromatin remodeling complex. Cell Mol Life Sci. 2015;72(13):2491-507. doi: 10.1007/s00018-015-1880-8. PubMed PMID: 25796366.
11. Eisen JA, Sweder KS, Hanawalt PC. Evolution of the SNF2 family of proteins: subfamilies with distinct sequences and functions. Nucleic Acids Res. 1995;23:2715-23.
12. Zhuang T, Hess RA, Kolla V, Higashi M, Raabe TD, Brodeur GM. CHD5 is required for spermiogenesis and chromatin condensation. Mech Dev. 2014;131:35-46. doi: 10.1016/j.mod.2013.10.005. PubMed PMID: 24252660; PubMed Central PMCID: PMCPMC3965579.
13. Bergs JW, Neuendorff N, van der Heijden G, Wassenaar E, Rexin P, Elsasser HP, et al. Differential expression and sex chromosome association of CHD3/4 and CHD5 during spermatogenesis. PLoS One. 2014;9(5):e98203. Epub 2014/05/23. doi: 10.1371/journal.pone.0098203. PubMed PMID: 24849318; PubMed Central PMCID: PMCPMC4029951.
14. Broering TJ, Alavattam KG, Sadreyev RI, Ichijima Y, Kato Y, Hasegawa K, et al. BRCA1 establishes DNA damage signaling and pericentric heterochromatin of the X chromosome in male meiosis. J Cell Biol. 2014;205(5):663-75. Epub 2014/06/11. doi: 10.1083/jcb.201311050. PubMed PMID: 24914237; PubMed Central PMCID: PMCPMC4050732.
15. Cafe SL, Skerrett-Byrne DA, De Oliveira CS, Nixon B, Oatley MJ, Oatley JM, et al. A regulatory role for CHD4 in maintenance of the spermatogonial stem cell pool. Stem Cell Reports. 2021;16(6):1555-67. Epub 2021/05/08. doi: 10.1016/j.stemcr.2021.04.003. PubMed PMID: 33961790; PubMed Central PMCID: PMCPMC8190575.
16. Costoya JA, Hobbs RM, Barna M, Cattoretti G, Manova K, Sukhwani M, et al. Essential role of Plzf in maintenance of spermatogonial stem cells. Nat Genet. 2004;36(6):653-9. Epub 2004/05/25. doi: 10.1038/ng1367. PubMed PMID: 15156143.
17. Buaas FW, Kirsh AL, Sharma M, McLean DJ, Morris JL, Griswold MD, et al. Plzf is required in adult male germ cells for stem cell self-renewal. Nat Genet. 2004;36(6):647-52. Epub 2004/05/25. doi: 10.1038/ng1366. PubMed PMID: 15156142.
18. Margolin G, Khil PP, Kim J, Bellani MA, Camerini-Otero RD. Integrated transcriptome analysis of mouse spermatogenesis. BMC Genomics. 2014;15:39. doi: 10.1186/1471-2164-15-39. PubMed PMID: 24438502; PubMed Central PMCID: PMCPMC3906902.

19. Nitarska J, Smith JG, Sherlock WT, Hillege MM, Nott A, Barshop WD, et al. A Functional Switch of NuRD Chromatin Remodeling Complex Subunits Regulates Mouse Cortical Development. Cell Rep. 2016;17(6):1683-98. doi: 10.1016/j.celrep.2016.10.022. PubMed PMID: 27806305; PubMed Central PMCID: PMCPMC5149529.
20. Gallardo T, Shirley L, John GB, Castrillon DH. Generation of a germ cell-specific mouse transgenic Cre line, Vasa-Cre. Genesis. 2007;45(6):413-7. Epub 2007/06/07. doi: 10.1002/dvg.20310. PubMed PMID: 17551945; PubMed Central PMCID: PMC2597027.
21. Zhang T, Oatley J, Bardwell VJ, Zarkower D. DMRT1 Is Required for Mouse Spermatogonial Stem Cell Maintenance and Replenishment. PLoS Genet. 2016;12(9):e1006293. Epub 2016/09/02. doi: 10.1371/journal.pgen.1006293. PubMed PMID: 27583450; PubMed Central PMCID: PMCPMC5008761.
22. Li W, Wu J, Kim SY, Zhao M, Hearn SA, Zhang MQ, et al. Chd5 orchestrates chromatin remodelling during sperm development. Nat Commun. 2014;5:3812. doi: 10.1038/ncomms4812. PubMed PMID: 24818823; PubMed Central PMCID: PMCPMC4151132.
23. Matson CK, Murphy MW, Griswold MD, Yoshida S, Bardwell VJ, Zarkower D. The mammalian doublesex homolog DMRT1 is a transcriptional gatekeeper that controls the mitosis versus meiosis decision in male germ cells. Dev Cell. 2010;19(4):612-24. Epub 2010/10/19. doi: 10.1016/j.devcel.2010.09.010. PubMed PMID: 20951351; PubMed Central PMCID: PMCPMC2996490.
24. Suzuki H, Ahn HW, Chu T, Bowden W, Gassei K, Orwig K, et al. SOHLH1 and SOHLH2 coordinate spermatogonial differentiation. Dev Biol. 2012;361(2):301-12. Epub 2011/11/08. doi: 10.1016/j.ydbio.2011.10.027. PubMed PMID: 22056784; PubMed Central PMCID: PMCPMC3249242.
25. Williams CJ, Naito T, Arco PG, Seavitt JR, Cashman SM, De Souza B, et al. The chromatin remodeler Mi-2beta is required for CD4 expression and T cell development. Immunity. 2004;20(6):719-33. Epub 2004/06/11. doi: 10.1016/j.immuni.2004.05.005. PubMed PMID: 15189737.
26. Oatley JM, Brinster RL. Spermatogonial stem cells. Methods Enzymol. 2006;419:259-82. Epub 2006/12/05. doi: 10.1016/S0076-6879(06)19011-4. PubMed PMID: 17141059.
27. Hammoud SS, Low DH, Yi C, Lee CL, Oatley JM, Payne CJ, et al. Transcription and imprinting dynamics in developing postnatal male germline stem cells. Genes Dev. 2015;29(21):2312-24. Epub 2015/11/08. doi: 10.1101/gad.261925.115. PubMed PMID: 26545815; PubMed Central PMCID: PMCPMC4647563.
28. Gassei K, Valli H, Orwig KE. Whole-mount immunohistochemistry to study spermatogonial stem cells and spermatogenic lineage development in mice, monkeys, and humans. Methods Mol Biol. 2014;1210:193-202. Epub 2014/09/01. doi: 10.1007/978-1-4939-1435-7_15. PubMed PMID: 25173170.

Figures

Figure 1

CHD4 expression and formation of different NURD complexes during gametogenesis. (A) Expression of *Chd4* monitored by immunofluorescence in testis sections of 14 dpp and 2 months (adult) old mouse using two distinct antibodies against CHD4, a rabbit polyclonal anti-CHD4 and anti-PLZF (top panel) and mouse monoclonal anti-CHD4 and anti-SOX9 (bottom panel). Arrows indicate examples of CHD4 positive spermatogonia (PLZF) or Sertoli (SOX9) cells. Cells within the punctuated line are pachytene spermatocytes. Similar results were observed using three different mice. **(B)** Western blot analysis of different NURD components in samples of cells enriched in undifferentiated spermatogonia (THY1.2+) (PLZF positive), differentiating spermatogonia (c-KIT+) (STRA8 positive) and the flow-through (FT), the latter from the spermatogonia enrichment procedure, which contains mostly somatic cells, including a large amount of Sertoli cells (SOX9 positive). Lamin B (Lam B) and a-tubulin (Tub.) were used as loading standards. The scheme represents the composition of a canonical NURD complex. **(C)** CHD4-participating NURD complexes in enriched fractions of spermatogonia or cells in the flow-through assessed by co-immunoprecipitation with anti-CHD4 as a bait. Non-specific IgG was used as a bait control. Experiments were repeated twice, and the star marks an unspecific reactive band.

Figure 2

***Chd4* and *Chd3* gene targeting design and testis developmental defects in *Chd4* mutant mice. (A and B)** Testis specific Cre knockout strategy for deletion of *Chd4* and *Chd3*. See description in Materials and Methods. **(C)** H&E-stained paraffin testis sections of wild type, Ddx4-*Chd4*$^{-/-}$, and Ddx4-*Chd3*$^{-/-}$ mice. **(D)** Quantification of testis weight for wild type and homozygous knockout mice is shown. Images and testis weigh measurements were obtained from three mice. **(E)** *Chd3* transcription levels were measured in Ddx4-*Chd3*$^{-/-}$ total testis and compared to wild type littermates (two months old mice, n=3). Chd4 transcription level in enriched fractions of spermatogonia obtained from 7 dpp Ddx4-*Chd4*$^{-/-}$ and control wild type litter mate mice (mice, biological replicate n=3).

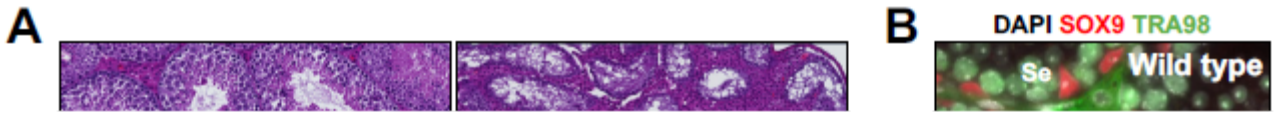

Figure 3

Ddx4-*Chd4*$^{-/-}$ mice show profound defects in gametogenesis. (A) H&E-stained histological sections of wild type and Ddx4-*Chd4*$^{-/-}$ testis. Stars mark seminiferous tubules with absent germ cells. Note unchanged number and morphology of Sertoli cells (indicated by green arrows). **(B)** Histological sections of wild type and Ddx4-*Chd4*$^{-/-}$ testis showing seminiferous tubules immunolabeled with SOX9 (a marker of Sertoli cells) and TRA98 (to mark germ cells). P, pachytene cells; Se, Sertoli cells; Rs, rounded spermatids. **(C)** H&E-stained histological sections of wild type and Ddx4-*Chd4*$^{-/-}$ ovaries. F, follicles and CL, corpora lutea.

Figure 4

Spermatogonia cell survival requires CHD4. (A) Histological sections of wild type and Ddx4-*Chd4*$^{-/-}$ testis cord from 9 days old mice stained with H&E (a and b) and Hematoxylin and immunostained with STRA8

antibodies (marking differentiating spermatogonia) (c and d). Arrows mark type of cells present in wild type but reduced in number or absent in the mutant. Experiments were done in at least three different mice showing similar results. **(B)** Immunostaining of sections of developing testis reveals severe loss of germ cells (TRA98) in *Chd4*$^{-/-}$ testis cords. **(C)** Quantitation of number of cell positive for TRA98, PLZF, and SOX9. *4dpp testis* (PLZF, wild type, 9.9 ± 4.1, n=47 seminiferous tubules; *Chd4*$^{-/-}$ 2.2 ± 1.4, n=56, P<0.0001, t test. TRA98, wild type 12.6 ± 5.3, n=35; *Chd4*$^{-/-}$ *3.0* ± 1.9, n=37, P<0.0001, t test). *7dpp testes* (PLZF, wild type, 14.6 ± 5.0, n=28; *Chd4*$^{-/-}$ 3.4 ± 2.4, n=45, P<0.0001, t test. TRA98, wild type 19.6 ± 5.9, n=48; *Chd4*$^{-/-}$ *3.0* ± 2.1, n=24, P<0.0001, t test). Experiments were done in three different mice showing similar results combined in our quantification. **(D)** Higher cell death in *Chd4*$^{-/-}$ knockout testes than in wild type controls at four days post-partum. Apoptotic cells were visualized by staining for TUNEL in three mice of each genotype. The percentage of apoptotic cells was counted only in the tubule cross-sections that contained apoptotic cells and was normalized to total number of germ cells. 19.05 ± 11.17, n = 468 (mean ± SD, n= number of seminiferous tubules counted) wild type and 38.25 ± 13.72 *Chd4*$^{-/-}$, n = 344; P<0.0001 (two-tailed Student t test). The arrows indicate apoptotic cells and arrowhead non-apoptotic germ cells.

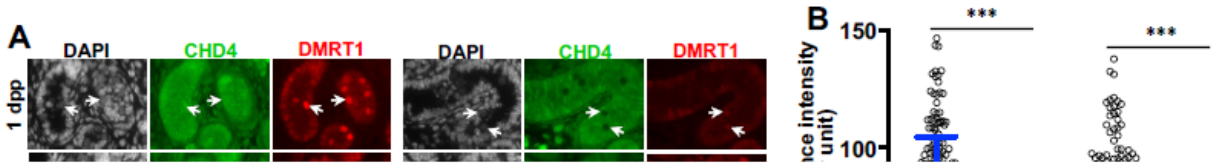

Figure 5

Effect of Chd4 deletion in Dmrt1 and Plzf expression. (A) Histological sections of wild type and Ddx4-*Chd4*$^{-/-}$ testis from 1, 4, and 7 dpp mice stained with CHD4 and DMRT1 antibodies. Arrows indicate examples of CHD4 positive spermatogonia (Wt) or CHD4 absence of staining in Ddx4-*Chd4*$^{-/-}$ spermatogonia and the correspondent cell stained for DMRT1. **(B)** Quantitation of fluorescence intensity of DMRT1 expression on spermatogonia is shown for wild type (Wt) and Ddx4-*Chd4*$^{-/-}$ knockout at ages of 1 dpp (Wt = 82.17 ± 22.02, n=272; and KO = 37.20 ± 10.01, n=287, P<0.0001, Student t test) and 4 dpp (Wt = 71.09 ± 20.93, n=242; and KO = 43.47 ± 14.88, n=198, P<0.0001, Student t test). Values represent the median fluorescence intensity ± standard deviation, n = total number of cells analyzed from 3 biological replicates using 3 different mice. (**C**) Histological sections of wild type and Ddx4-*Chd4*$^{-/-}$ testis from 1, 4, and 7 dpp mice stained with antibodies against PLZF. **(D)** Quantitation of fluorescence intensity of PLZF expression on spermatogonia is shown for wild type and Ddx4-*Chd4*$^{-/-}$ knockout at ages of 1 dpp (wt = 17.94 ± 4.10, n=300; and Ddx4-*Chd4*$^{-/-}$ = 10.89 ± 4.07, n=339, P<0.0001, Student t test) and 4 dpp (Wt = 17.78 ± 4.70, n=282; and Ddx4-*Chd4*$^{-/-}$ = 9.11 ± 3.75, n=230, P<0.0001, Student t test). Values represent the median fluorescence intensity ± standard deviation, n = total number of cells analyzed from 3 biological replicates using 3 different mice. **(E)** Diagram representing CHD4, Dmrt1, and Plzf relationship in spermatogonia stem cell maintenance. Note that our studies do not address the possibility that Plzf may be a direct target of CHD4.

Supplementary Files

This is a list of supplementary files associated with this preprint. Click to download.

- FigS1.pdf
- FigS2.pdf
- FigS3.pdf
- FigS4.pdf
- FigS5.pdf
- FigS6.pdf
- FigS7.pdf
- SupplementaryFigurelegend.docx
- TableS1Antibodies.docx